Entropic multiple–relaxation–time lattice Boltzmann models

Pietro Asinari, PhD

Dipartimento di Energetica, Politecnico di Torino, Torino, Italy,
e-mail: pietro.asinari@polito.it,
home page: http://staff.polito.it/pietro.asinari

joint work with Ilya V. Karlin, PhD

Institute of Energy Technology, ETH Zurich, Switzerland
School of Engineering Sciences, University of Southampton, UK

Outline of this talk

1. Preliminaries
   - Motivation and notation
   - The Maxwellian state
2. The key results
   - The generalized Maxwellian state
   - The constrained Maxwellian state
3. Derivation of kinetic models
   - Entropic model with blended pressure tensor (EMRT)
   - Entropic model with blended population (EQE)
4. Numerical validation
   - Taylor–Green vortex flow
   - Lid driven cavity

Outline Compass

Motivation

- The goal is to improve the stability of the Lattice Boltzmann (LB) schemes with regards to rough meshes, but preserving the required level of accuracy.
- In recent years, two approaches have been developed for the previous goal:
    1. the multiple–relaxation–time (MRT) schemes with tunable bulk viscosity, which is a free parameter to dump the compressibility error, when searching for the incompressible limit;
    2. the entropic (ELB) schemes, which admit analytical equilibria ensuring the existence of the H–theorem by construction.
- There are some controversies (!!) about the previous schemes: in order to settle them, the idea is to develop a new class of MRT schemes with both tunable bulk viscosity and H–theorem.
- The key result, which makes this possible, is a brand new analytical generalized Maxwellian for discrete lattices.

Notation

- Let us consider the D2Q9 lattice: $\boldsymbol{v}_0 = (0,\, 0)$, $\boldsymbol{v}_\alpha = (\pm c,\, 0)$ and $(0,\, \pm c)$ for $\alpha =$ 1–4, and $\boldsymbol{v}_\alpha = (\pm c,\, \pm c)$ for $\alpha =$ 5–8, where c is the lattice spacing.
- The D2Q9 lattice derives from the three–point Gauss–Hermite formula, with the following weights $w(-1) = 1/6$, $w(0) = 2/3$ and $w(+1) = 1/6$.
- Let us arrange in the list v_x (v_y) all the components of the lattice velocities along the x–axis (y–axis) and in the list f all the populations f_α. Algebraic operations for the lists are always assumed component-wise.
- The sum of all the elements of the list p is denoted by $\langle p \rangle = \sum_{i=0}^{Q-1} p_i$. The dimensionless density ρ, the flow velocity $\boldsymbol{u}$ and the pressure tensor $\boldsymbol{\Pi}$ are defined by $\rho = \langle f \rangle$, $\rho u_i = \langle v_i f \rangle$ and $\rho \Pi_{ij} = \langle v_i\, v_j\, f \rangle$ respectively.

Local equilibrium: Maxwellian state

- The convex entropy function (H–function) for this lattice is [1]

$$H(f) = \langle f \, \ln (f/W) \rangle, \tag{1}$$

where $W = w(v_x)\, w(v_y)$ and the equilibrium population list is

Definition of Maxwellian state (f_M)

$f_M = \min_{f \in \mathsf{P}_M} H(f)$, where P_M is the set of functions such that $\mathsf{P}_M = \{ f > 0 : \langle f \rangle = \rho, \; \langle \boldsymbol{v} f \rangle = \rho \boldsymbol{u} \}$

- Minimization of the H–function under the constraints of mass and momentum conservation yields [2]

$$f_M = \rho \prod_{i=x,y} w(v_i) \left(2 - \varphi(u_i/c)\right) \left(\frac{2(u_i/c) + \varphi(u_i/c)}{1 - (u_i/c)} \right)^{v_i/c}, \tag{2}$$

where $\varphi(z) = \sqrt{3z^2 + 1}$. In order to ensure the positivity of f_M, the low Mach number limit must be considered, i.e. $|u_i| < c$.

Outline Compass

Local quasi–equilibrium: generalized Maxwellian state

- Let us introduce a novel quasi–equilibrium [3, 4, 5] population list, by requiring, in addition, that the diagonal components of the pressure tensor $\mathbf{\Pi}$ have some prescribed values, namely

Definition of generalized Maxwellian state (f_G)

$f_G = \min_{f \in \mathsf{P}_G} H(f)$, where $\mathsf{P}_G \subset \mathsf{P}_M$ is the set of functions such that $\mathsf{P}_G = \left\{ f > 0 : \langle f \rangle = \rho,\ \langle \boldsymbol{v} f \rangle = \rho \boldsymbol{u},\ \langle v_i^2 f \rangle = \rho \Pi_{ii} \right\}$.

- In other words, minimization of the H–function under the constraints of mass and momentum conservation and prescribed diagonal components of the pressure tensor yields

$$f_G = \rho \prod_{i=x,y} w(v_i)\, \frac{3\,(c^2 - \Pi_{ii})}{2\,c^2} \left(\sqrt{\frac{\Pi_{ii} + c\,u_i}{\Pi_{ii} - c\,u_i}} \right)^{v_i/c} \left(\frac{2\sqrt{\Pi_{ii}^2 - c^2\,u_i^2}}{c^2 - \Pi_{ii}} \right)^{v_i^2/c^2} . \tag{3}$$

The plane of parameters

- In order to ensure the positivity of f_G, we use $\Pi = (\Pi_{xx}, \Pi_{yy}) \in \Omega$ for a generic point on the two-dimensional plane of parameters $\Omega = \{\Pi : c\,|u_x| < \Pi_{xx} < c^2,\ c\,|u_y| < \Pi_{yy} < c^2\}$.

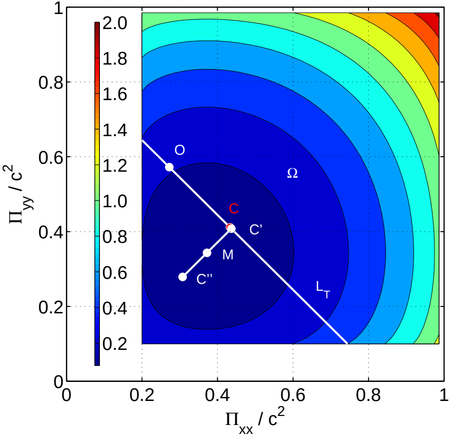

The H–function in the generalized Maxwell states

- It is possible to evaluate explicitly the H–function in the generalized Maxwell states (3), $H_G = H\left(f_G\right)$, the result is written

$$H_G = \rho \ln \rho + \rho \sum_{i=x,\,y} \sum_{k=-,\,0,\,+} w_k \, a_k(\Pi_{ii}) \ln \left(a_k(\Pi_{ii}) \right), \qquad (4)$$

  where $w_{\pm} = w(\pm 1)$, $w_0 = w(0)$, $a_{\pm}(\Pi_{ii}) = 3\,(\Pi_{ii} \pm c\,u_i)/c^2$ and $a_0(\Pi_{ii}) = 3\,(c^2 - \Pi_{ii})/(2\,c^2)$.
- Generalizing the result [6], let us derive a constrained equilibrium f_C which brings the H-function to a minimum among all the population lists with a prescribed trace $T(\mathbf{\Pi}) = \Pi_{xx} + \Pi_{yy}$, namely

Definition of constrained Maxwellian state (f_C)

Given $\{f_G\}$ the set of generalized Maxwellian states with trace T, then $f_C \in \{f_G\}$ is such that $\left[(\partial H_G / \partial \Pi_{xx}) - (\partial H_G / \partial \Pi_{yy})\right]_{(\Pi_{xx}+\Pi_{yy}=T)} = 0$.

The constrained Maxwellian state

- The solution to the latter problem exists and yields a cubic equation in terms of the normal stress difference $N = \Pi^C_{xx} - \Pi^C_{yy}$,

$$N^3 + a\,N^2 + b\,N + d = 0,$$
$$a = -\frac{1}{2}\,(u_x^2 - u_y^2),\;\; b = (2\,c^2 - T)\,(T - u^2),$$
$$d = -\frac{1}{2}\,(u_x^2 - u_y^2)\,(2\,c^2 - T)^2. \tag{5}$$

- Let us define $p = -a^2/3 + b$, $q = 2\,a^3/27 - a\,b/3 + d$ and $\Delta = (q/2)^2 + (p/3)^3$. For $\Delta \geq 0$, the Cardano formula implies

$$\Pi^C_{xx} = \frac{T}{2} + \frac{1}{2}\left(r - \frac{p}{3\,r} - \frac{a}{3}\right),\;\; r = \sqrt[3]{-\frac{q}{2} + \sqrt{\Delta}}, \tag{6}$$

while $\Pi^C_{yy} = T - \Pi^C_{xx}$. Thus, substituting (6) into (3), we find

$$f_C = f_G(\rho, \boldsymbol{u}, \Pi^C_{xx}(\boldsymbol{u}, T), \Pi^C_{yy}(\boldsymbol{u}, T)). \tag{7}$$

Outline Compass

Entropic model with blended pressure tensor (EMRT)

- By means of the usual equilibrium M and the newly found constrained equilibrium C, let us define the generalized equilibrium $E(\beta) = \left(\Pi^E_{xx}(\beta), \Pi^E_{yy}(\beta)\right)$ as a linear interpolation between the points M and C on the Ω plane

$$E(\beta) = \beta\, M + (1-\beta)\, C, \tag{8}$$

where β is a free parameter (see next for its admissible range).

- Thus, the generalized equilibrium list is defined as

$$f_{GE}(\beta) = f_G(\rho, \boldsymbol{u}, \Pi^E_{xx}(\beta), \Pi^E_{yy}(\beta)). \tag{9}$$

- Considering kinetic equation of the form, $\partial_t f + \boldsymbol{v} \cdot \partial_{\boldsymbol{x}} f = J(f)$, let us define the following collision operator

$$J(f) = \lambda \left[f_{GE}\,(\beta) - f \,\right], \tag{10}$$

where $\lambda > 0$ is a parameter, ruling the relaxation toward the generalized equilibrium. In the continuum limit, λ is related to the kinematic viscosity.

Proof of the H–theorem for EMRT model

H–theorem for EMRT model

The production σ due to the relaxation term (10), where $\sigma = \langle \ln(f/W)\, J(f) \rangle$, is non-positive and it annihilates at the equilibrium, i.e. $\sigma(f_M) = 0$, if $0 < \beta \leq \beta^*$ where $\beta^*(f)$.

Proof [part 1 of 2]

Because of the convexity of the H-function and because $f_G(\Pi_{xx}, \Pi_{yy})$ minimizes H among all the lists with the moments (Π_{xx}, Π_{yy})

$$\frac{\sigma}{\lambda} \leq H_{GE}(\beta) - H(f) \leq H_{GE}(\beta) - H_G(\Pi), \tag{11}$$

where $H_{GE}(\beta) = H_G\left(\Pi^E_{xx}(\beta), \Pi^E_{yy}(\beta)\right)$. Recalling that $\mathbf{\Pi}(f_{GE}(0))$ and $\mathbf{\Pi}(f_G(\Pi_{xx}, \Pi_{yy}))$ have the same trace, inequality (11) can be rewritten

$$\frac{\sigma}{\lambda} \leq H_{GE}(\beta) - H_{GE}(0) + H_{GE}(0) - H_G(\Pi) \leq H_{GE}(\beta) - H_{GE}(0).$$

Proof of the H–theorem for EMRT model

Proof [part 2 of 2]

- What remains to estimate is the range of β such that $H_{GE}(\beta) \leq H_{GE}(0)$. Clearly, since $M = E(1)$ is the absolute minimum of H_G, and because $H_{GE}(\beta)$ is a convex function, σ is non-positive if $0 < \beta \leq 1$.
- In order to extend the proof to $\beta > 1$, let us consider the entropy estimate [1]:

$$H_{GE}(\beta^*) = H_{GE}(0). \tag{12}$$

Thanks to the convexity of $H_{GE}(\beta)$, the non-trivial solution $\beta^* > 1$ to this equation is unique when it exists. In the opposite case, we need to take care of the boundary of the positivity domain Ω. In both cases, for $0 < \beta \leq \beta^*$, it holds $H_{GE}(\beta) \leq H_{GE}(0)$ and thus the entropy production is non-positive, $\sigma \leq 0$.

■

Graphical interpretation of the H–theorem

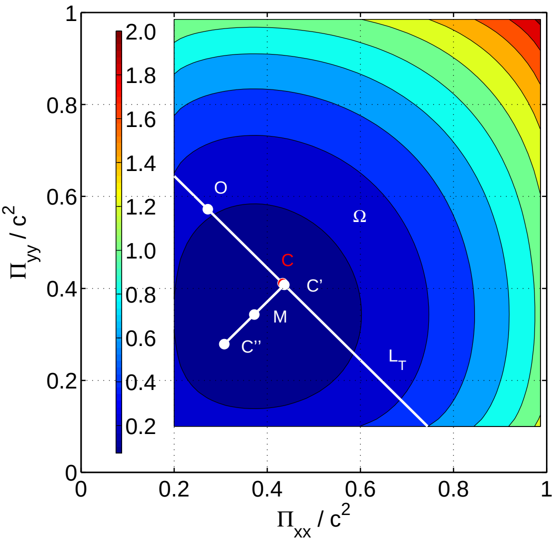

Switching the interpolation strategy

- Introducing a linear mapping for computing the moments, namely

$$M = \left[1,\, v_x,\, v_y,\, v_x^2,\, v_y^2,\, v_x v_y,\, v_x^2 v_y,\, v_x v_y^2,\, v_x^2 v_y^2\right]^T, \tag{13}$$

and recalling that

$$m_G = M \cdot f_G = \rho\left[1,\, u_x,\, u_y,\, \Pi_x,\, \Pi_y,\, u_x u_y,\, u_y \Pi_x,\, u_x \Pi_y,\, \Pi_x \Pi_y\right]^T,$$

it is possible to realize that the moments m_G of the generalized Maxwellian state f_G are linear with regards to the prescribed pressure components up to the third order.

- Hence the previous linear interpolation of the pressure tensor components between the points M and C, namely

$$\Pi_{ii}(\beta) = \beta\, \Pi_{ii}^M + (1-\beta)\, \Pi_{ii}^C, \qquad \text{for} \;\; i = x, y, \tag{14}$$

is equivalent to a linear interpolation of the population lists

$$f_{QE}(\beta) = \beta\, f_M(\rho, \boldsymbol{u}) + (1-\beta)\, f_C(\rho, \boldsymbol{u}, \Pi_{xx} + \Pi_{yy}), \tag{15}$$

up to the third order included.

Entropic model with blended population (EQE)

- Let us define the following new collision operator

$$J_Q(f) = \lambda \left[f_{QE}(\beta) - f \right], \tag{16}$$

or equivalently, introducing $\tau_f = 1/\lambda$ and $\tau_s = \tau_f/\beta$,

$$J_Q(f) = -\frac{1}{\tau_f}(f - f_C) - \frac{1}{\tau_s}(f_C - f_M). \tag{17}$$

- In the previous model, the relaxation to the equilibrium is split in two steps. In the first step, the population list f relaxes to the constrained equilibrium f_C with the relaxation time τ_f (fast mode). In the second step, the constrained equilibrium relaxes to the equilibrium with the second relaxation time τ_s (slow mode) [7].
- The previous model can also be expressed as

$$J_Q(f) = -\frac{1}{\tau_s}(f - f_M) - \frac{\tau_s - \tau_f}{\tau_f \tau_s}(f - f_C). \tag{18}$$

Proof of the H–theorem for EQE model

H–theorem for EQE model

The production σ_Q due to the relaxation term (17), where $\sigma_Q = \langle \ln(f/W) J_Q(f) \rangle$, is non-positive and it annihilates at the equilibrium, i.e. $\sigma_Q(f_M) = 0$, if $0 < \tau_f \leq \tau_s$ (same as $0 < \beta \leq 1$).

Proof

Recalling Eq. (18) yields

$$\sigma_Q = -\frac{1}{\tau_s} \langle \ln(f/f_M)(f - f_M) \rangle - \frac{\tau_s - \tau_f}{\tau_f \tau_s} \langle \ln(f/f_C)(f - f_C) \rangle, \quad (19)$$

which is non–positive and semi–definite provided that relaxation times satisfy the condition

$$\tau_f \leq \tau_s.$$

■

Outline Compass

Numerical implementation

- Applying the following variable transformation, namely

$$f \to g = f - \delta t \, J_Q/2, \tag{20}$$

(δt is the time step) to the EQE discrete velocity model yields

$$g(\boldsymbol{x} + \boldsymbol{c}\delta t, t + \delta t) = (1 - \omega_f) g(\boldsymbol{x}, t) + \omega_f f_{QE}(\rho, \boldsymbol{u}, T'), \tag{21}$$

where $1/\omega_f = \tau_f/\delta t + 1/2$, where as usual $\rho = \langle g \rangle$ and $\rho u_i = \langle c_i g \rangle$, but, since the trance is not conserved,

$$T' = (1 - \omega_s/2)\, T(g) + \omega_s T_M(g)/2,$$

where $1/\omega_s = \tau_s/\delta t + 1/2$ and

$$T(g) = \langle (c_x^2 + c_y^2) g \rangle, \qquad T_M(g) = 2/3 \left[\varphi(u_x/c) + \varphi(u_y/c) - 1 \right].$$

- By means of asymptotic analysis, it is possible to prove that the previous EQE model recovers the Navier–Stokes equations up to the second order w.r.t. $\delta x = c\,\delta t$, with a kinematic viscosity $\nu = \tau_f/3$ and a bulk viscosity $\xi = \tau_s/3$.

Taylor–Green vortex flow

- First of all, let us verify the transport coefficients by means of the analytical solution for the Taylor–Green vortex flow.

	ξ/ν	ν	Measured ν	Error [%]
BGK	1	0.001	0.00102065	2.06
EQE	10	0.001	0.00102071	2.07
EQE	100	0.001	0.00102106	2.11
BGK	1	0.010	0.00998509	-0.15
EQE	10	0.010	0.00998555	-0.14
EQE	100	0.010	0.00998654	-0.13
BGK	1	0.100	0.09977323	-0.23
EQE	10	0.100	0.09977355	-0.23
EQE	100	0.100	0.09977230	-0.23

- In the low Mach limit, the slow relaxation frequency τ_s, controlling the bulk viscosity, does not effect the leading part of the solution.

Lid driven cavity at Re $= 1000$: streamlines

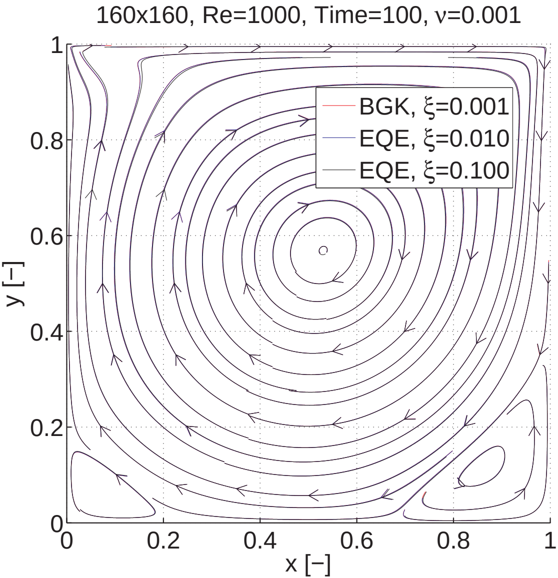

Lid driven cavity at Re $= 1000$: pressure contours

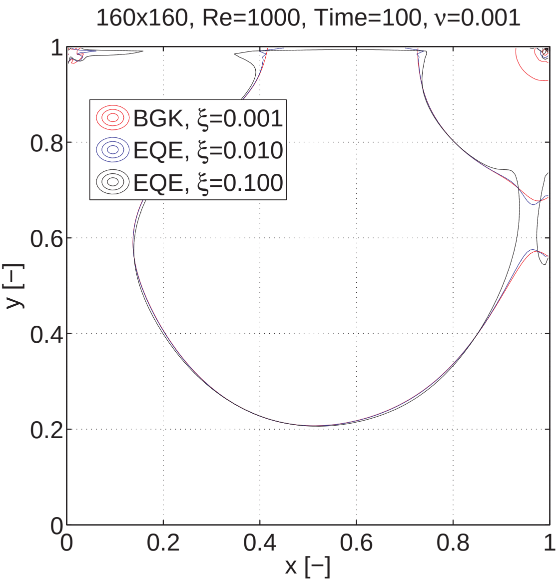

Lid driven cavity: stability enhancement

- Let us assume $\xi = 10\,\nu$ for enhancing the stability of EQE.

		BGK		EQE $\xi = 10\,\nu$	
Re	ν	$\min(N)$	$\max$ (Ma)	$\min(N)$	$\max$ (Ma)
1000	1.0×10^{-3}	50	0.2	25	0.4
2000	5.0×10^{-4}	100	0.2	50	0.4
3000	3.3×10^{-4}	150	0.2	75	0.4
4000	2.5×10^{-4}	200	0.2	100	0.4
5000	2.0×10^{-4}	250	0.2	125	0.4

- Effectively this choice allows one to perform calculations with rougher meshes $N \times N$ or (equivalently) higher Mach numbers (Ma $= 0.01$ Re Kn was adopted).
- However the previous consideration does not lead automatically to a performance improvement, because the accuracy must be considered as well.

Lid driven cavity at Re $= 5000$: main vortexes

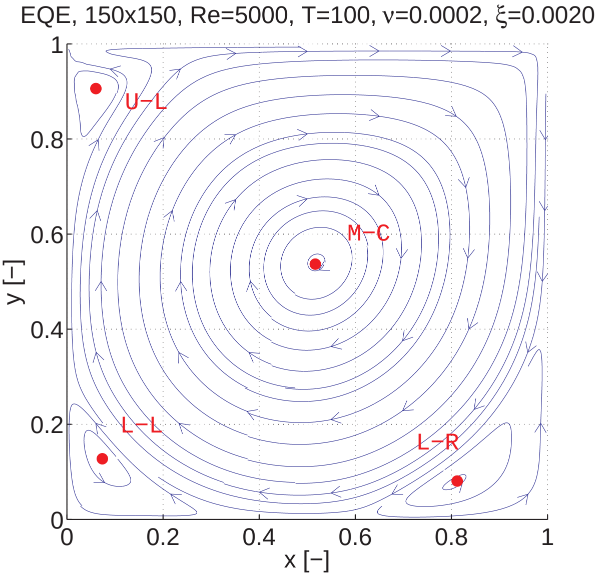

Lid driven cavity at Re $= 5000$: stability vs. accuracy

- Let us compute the locations of the main vortexes [8, 9, 10, 11].

	Run time	Errors on vortex locations [%] M-C	L-L	L-R	U-L	Mean
EQE 125×125	0.35	1.15	12.41	1.61	1.36	4.13
EQE 150×150	0.61	0.74	12.41	2.29	0.49	3.98
EQE 170×170	1.00	1.20	6.93	2.29	0.63	2.76
EQE 200×200	2.06	1.10	4.51	1.81	0.06	1.87
EQE 250×250	4.97	1.10	2.24	2.35	0.06	1.44
ELB [12] 320×320	???	0.48	6.35	2.09	0.22	2.29
BGK 250×250	2.84	1.16	7.76	1.88	0.06	2.72

- The key result is that the EQE model, with a rougher mesh $170^2 \sim 250^2/2$ than that used by the BGK model, can achieve the same accuracy (2.76% $\sim$ 2.72%).
- This gives to the EQE model an effective computational speed-up of 2.84 times over the BGK model (!!).

Lid driven cavity at Re $= 5000$: EQE vs. BGK

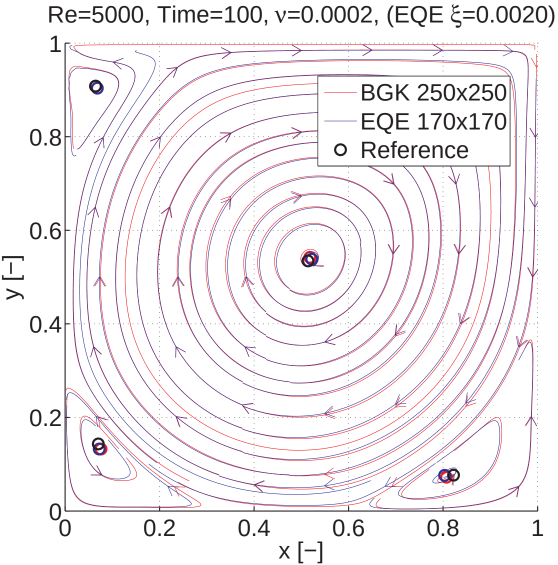

Conclusions

- Some brand new analytical results for discrete lattices have been presented: in particular, the generalized Maxwellian state f_G (with prescribed diagonal components of the pressure tensor) and the constrained Maxwellian state f_C (with prescribed trace of the pressure tensor).
- All the previously introduced equilibria for LB are found as special cases of the previous results (!!).
- Some new LB schemes (EMRT and EQE) with both tunable bulk viscosity and H–theorem have been reported.
- In case of lid driven cavity test, the EQE model was able to achieve the same accuracy of the usual BGK model with a rougher mesh (approximately half), leading to a remarkable speed–up of the run time (even though both codes were not optimized !!).

- Thank you !!

References I

[1] I. V. Karlin, A. Ferrante, and H. C. Ottinger
Europhys. Lett., 47:182, 1999.

[2] S. Ansumali, I. V. Karlin, and H. C. Ottinger
Europhys. Lett., 63:798, 2003.

[3] A. N. Gorban, I. V. Karlin,
Physica A, 206:401, 1994.

[4] C. D. Levermore,
J. Stat. Phys., 83:1021, 1996.

[5] A. N. Gorban, and I. V. Karlin
Invariant Manifolds for Physical and Chemical Kinetics
in Lecture Notes in Physics
Springer-Verlag, Berlin, 2005.

[6] S. Ansumali, and I. V. Karlin,
Phys. Review Lett., 95:260605, 2005.

[7] S. Ansumali, S. Arcidiacono, S. S. Chikatamarla,
N. I. Prasianakis, A. N. Gorban, and I. V. Karlin
Eur. Phys. J. B, 56:135, 2007.

References II

[8] U. Ghia, K.N. Ghia, and C.Y. Shin
J. Comput. Phys., 48:387, 1982.

[9] R. Schreiber and H.B. Keller,
J. Comput. Phys., 49:310, 1983.

[10] S.P. Vanka
J. Comput. Phys., 65:138, 1986.

[11] S. Hou, Q. Zou, S. Chen, G. D. Doolen, and A. C. Cogley
J. Comput. Phys., 118:329, 1995.

[12] S. Ansumali, and I. V. Karlin,
Phys. Review E, 65:056312, 2002.